Journal of Arid Environments 100-101 (2014) 31–41

Contents lists available at ScienceDirect

Journal of Arid Environments

journal homepage: www.elsevier.com/locate/jaridenv

Quantifying the contributions of agricultural oasis expansion, management practices and climate change to net primary production and evapotranspiration in croplands in arid northwest China

J. Bai [a], X. Chen [a], L. Li [a,*], G. Luo [a], Q. Yu [b]

[a] State Key Laboratory of Desert and Oasis Ecology, Xinjiang Institute of Ecology and Geography, Chinese Academy of Sciences, Urumqi 830011, China
[b] Plant Functional Biology & Climate Change Cluster, University of Technology, Sydney, PO Box 123, Broadway, NSW 2007, Australia

ARTICLE INFO

Article history:
Received 11 October 2012
Received in revised form
23 September 2013
Accepted 4 October 2013
Available online 27 October 2013

Keywords:
Biome-BGC model
Agricultural oasis
Human activities
Carbon cycle
Water shortage

ABSTRACT

Cropland area in north-western China has quadrupled over the past 50 years. The effects of this rapid expansion on regional carbon and water budgets have not been examined quantitatively. In this study, an enhanced Biome-BGC model including crop growth processes was used to quantify the effects on regional net primary productivity (NPP) and evapotranspiration (ET) in a representative catchment. The model results were in good agreement with biometric measurements. The catchment-scale total NPP (TNPP) and total ET (TET) increased by 81.8% and 89.4%, respectively. The increase in cropland area (LUCC) explained 40.3% and 60.5% of the increased TNPP and TET, while management practices (Mana) accounted for 46.1% and 16.8% of the increased TNPP and TET, respectively. Climate change (CLM) had the least influence on the increase in TNPP and TET (accounting for 1.8% and 4.7%). As assuming no interactions between CLM and LUCC, we detected effects of interactions between CLM and Mana (accounting for 10% and 16.8%) and between Mana and LUCC (accounting for 1.8% and 4.7%) on the increased TNPP and TET. These results implied that the rapid expansion of cropland and intensive agricultural management practices had important effects on regional carbon and water budgets.

1. Introduction

Arid and semi-arid regions cover approximately one third of the world's land area (Okin et al., 2006). In China, these regions cover approximately 22% of the land area, 2.15×10^6 km^2, mostly in the northwestern part of the country (Hu et al., 2010). Agricultural oases are referred to cultivated land in arid or semi-arid regions formed by human activities that are irrigated by anthropogenic means (e.g., withdrawn river water or pumped underground water; Wang, 2010a,b). Agriculture in artificial oases is necessary to maintain social development and the increased population in these arid and semi-arid regions (Chen, 2008) and plays an important role in the regional carbon and water cycle (Foley et al., 2005). First, most agricultural cropland was converted from natural vegetation in natural oases, which are generally called agricultural oases in arid and semi-arid regions of northwest China. Thus, agriculture is highly dependent on management practices such as irrigation and fertilization (Wang and Zhang, 1999), which increase crop yields and modify the carbon, water, and nitrogen budgets in the cropland (Li et al., 2005; Zhang et al., 2011). Second, the arable area of the agricultural oases in northwestern China has quadrupled from 2.5×10^5 km^2 to 10.4×10^5 km^2 over the past 50 years (Wang, 2010a,b). The expansion of agricultural oases is a type of land-use and land-cover change (LUCC), which greatly changes the vegetation distribution and surface biogeochemical and biophysical processes, leading to dramatic changes in the water cycle and ecosystem productivity (Houghton and Hackler, 2003; Tian et al., 2011). At the same time, water is the most limiting resource for sustaining crop production in agricultural oases due to high water demands of the increased cropland area and population (Jia et al., 2004). To address this concern, the effects of expansion and associated management practices in agricultural oases on regional carbon and water budgets have not been examined quantitatively.

The effects of LUCC and agriculture on the terrestrial carbon cycle can be estimated based on the process-based terrestrial ecosystem models that have been widely used in recent decades (Bondeau et al., 2007; Ciais et al., 2011; Li et al., 2011; Parton et al., 1998; Vuichard et al., 2008), or based on statistically empirical models (Aggarwal et al., 2006; Bradford et al., 2005; Field et al., 1995; Graf et al., 1990; Huang et al., 2007; Lieth, 1975; Potter et al., 1993). Terrestrial ecosystem models can be used to describe

* Corresponding author. Tel.: +86 991 7885401.
E-mail addresses: lilhchn@gmail.com, lhli@ms.xjb.ac.cn (L. Li).

0140-1963/$ – see front matter
http://dx.doi.org/10.1016/j.jaridenv.2013.10.004

the effects of human activities and environmental changes on carbon balance in croplands based on geophysical and geochemical processes and, therefore, have received much more attention (Ciais et al., 2011). A large number of terrestrial ecosystem models have been developed, including the Biome-BGC (Running and Hunt, 1993), IBIS (Kucharik, 2003), ORCHIDEE (Krinner et al., 2005), and JULES (Clark et al., 2011) models. All of these models were originally designed for natural vegetation, not for crops. When the models are applied to agricultural systems, the crops are generally described as grasslands (Churkina et al., 2010; Gervois et al., 2004; Mu et al., 2008; Vetter et al., 2008; Wang et al., 2005); however, the crops differ from grasslands in both physiological processes and management practices (Gervois et al., 2004). Therefore, some terrestrial ecosystem models have been coupled with crop growth models. The Agro-IBIS model has incorporated managed agroecosystems into the IBIS model (Kucharik and Brye, 2003) and has been used to simulate the spatial patterns and impact on maize yield at the regional scale in the USA (Kucharik, 2003). Gervois et al. (2004) and De Noblet-Ducoudré et al. (2004) coupled the ORCHIDEE model with STICS, an agronomic crop-growth model, and Li et al. (2011) comprehensively assessed its performance in estimating the fluxes of CO_2 and H_2O in several European maize sites. Hoof et al. (2011) incorporated a generic crop model (SUCROS) into a land surface model (JULES) and evaluated the fluxes simulated by the coupled JULES-SUCROS model against FLUXNET measurements at six European sites. Crop-specific parameters and management practices are defined in these coupled models, and their effects on phenology, biomass allocation, and carbon and water processes are given in the ecosystem model (De Noblet-Ducoudré et al., 2004; Gervois et al., 2004; Kucharik and Brye, 2003).

The Biome-BGC (BioGeochemical Cycles) model is a common model that can be used to simulate the carbon, nitrogen and water cycles of terrestrial ecosystems (Running and Hunt, 1993). The Biome-BGC model is a multi-biome generalization of FOREST-BGC (Running and Coughlan, 1988), which was originally developed to simulate a forest's development through its life cycle. The Biome-BGC model has been widely used for various biomes, including forests (Chiesi et al., 2007), grasslands (Running and Hunt, 1993) and crops (treating them as grasslands; Wang et al., 2005) and has been used at the site (Ueyama et al., 2010), regional (Mu et al., 2008; Turner et al., 2007) continental and global scales (Churkina et al., 2010; Vetter et al., 2008). The Biome-BGC model has already been modified to simulate the carbon and water flux of agro-ecosystems. Di Vittorio et al. (2010) updated the Biome-BGC model (Agro-BGC) to investigate the carbon, nitrogen and water balance of C_4 perennial grasslands, including crops. Ma et al. (2011) used eddy flux measurements of agro-ecosystems to identify the spatially generalized ecophysiological parameters of the ANTHRO-BGC model (another modified version of the Biome-BGC) in croplands. Both versions of the modified Biome-BGC model have been used at the site scale; however, the crops were still treated as "managed grasslands", and specific features of crops' physiological processes such as phenology, biomass allocation and agricultural management practices were not described when the Biome-BGC model was used at the regional scale.

Therefore, the objectives of this study are to (1) incorporate a specific agricultural module including crop phenology, biomass allocation and agricultural management practices (irrigation and fertilization) into the Biome-BGC model; (2) evaluate the performance of the enhanced Biome-BGC in simulating crop biometric variables (leaf area index, LAI, leaf and stem biomass, grain yield) and evapotranspiration (ET); and (3) apply the modified Biome-BGC to a representatively agricultural oasis in northwest China to investigate the temporal-spatial changes in NPP and ET and to estimate the contributions of the increased area in agricultural oasis, management practices and climate change on regional NPP and ET from 1971 to 2006.

2. Material and methods

2.1. Study area

This study area was in Sangonghe Catchment, a relatively isolated in land catchment with mountains, agricultural oasis and deserts in the arid region of northwestern China (Fig. 1). The agricultural oasis is called Sangonghe Oasis and is located in the north Tianshan Mountains and southern flank of Junggar Basin, with total area of approximately 942 km^2. The upper alluvial fan, at an elevation of 500–700 m, has gravelly and sandy desert soil where corn was grown, while the lower alluvial plain, at an elevation of 450–500 m, has fine-textured clay soil in which the dominant crop is winter wheat (Luo et al., 2008). The climate is extremely dry, and precipitation during the growing season was not sufficient to meet the demands of crop growth. The mean annual solar radiation was 5650 W m^{-2}, and the annual average temperature was 6.9 °C from 1971 to 2006. The mean annual precipitation was only 226 mm, while the annual potential evaporation reached 1808 mm. The old oasis is distributed along the river edge, and the newly developed oasis is converted from the shrublands or grasslands in or around the original oasis. The water withdrawn from Sangonghe River and pumped from groundwater was used for irrigation in Sangonghe Oasis (Wang et al., 2008).

2.2. Biometric measurements

Biometric data (LAI, leaf and stem biomass, and grain yield) were collected at Wulanwusu Agrometeorological Station (WAS). WAS is located in a suburb of Shihezi city (44.3°N, 85.8°E, 468.5 m a.s.l.), 180 km from Fukang city, the center of the Sangonghe Catchment (Fig. 1). Biometric measurements were taken from 1995 to 2007. The WAS site has climatic conditions similar to those of Sangonghe Oasis. The mean annual temperature was 7.5 °C, annual precipitation was 225 mm, and annual pan evaporation was 1571 mm.

LAI and biomass (fresh and dry weights) were measured from destructive plant samples. Ten winter wheat plants were harvested at four stages including turning green, elongation, heading and milk-ripe stages; additionally, five corn plants were harvested at the three-leaf, seven-leaf, elongation, heading and milk-ripe stages. The number of winter wheat and maize was counted in each LAI measured periods in a 1 m × 1 m plot. Winter wheat had a higher plant density than corn. The maximum plant density of winter wheat and corn was 1390 plants m^{-2} and 12.5 plants m^{-2}, while the minimum value was 810 plants m^{-2} and 7.5 plants m^{-2}. The dimensions (length and width) of all the leaves of the sampled plants were measured with a scale, and the total leaf area was calculated as the product of its length along the primary vein, its maximum width and a correction coefficient (0.85 for winter wheat and 0.7 for corn). The leaf area per unit of single crop (unit: m^2 plants^{-1}) was converted to leaf area per unit of ground area (unit: m^2 m^{-2}) by plant density (unit: plants m^{-2}). Then, the sampled plants were divided into leaves and stems (including sheaths), and were oven-dried for 8–10 h. The dry matter of the leaves and stems were weighed separately. The mature crop plants in a 5 m × 5 m plot were harvested and oven-dried for 8–10 h, and the yield was measured by weighing the dried grains.

2.3. Management practice data

The mean dates of sowing in the Sangonghe Oasis for winter wheat and corn were 21 September and 21 April, while the mean

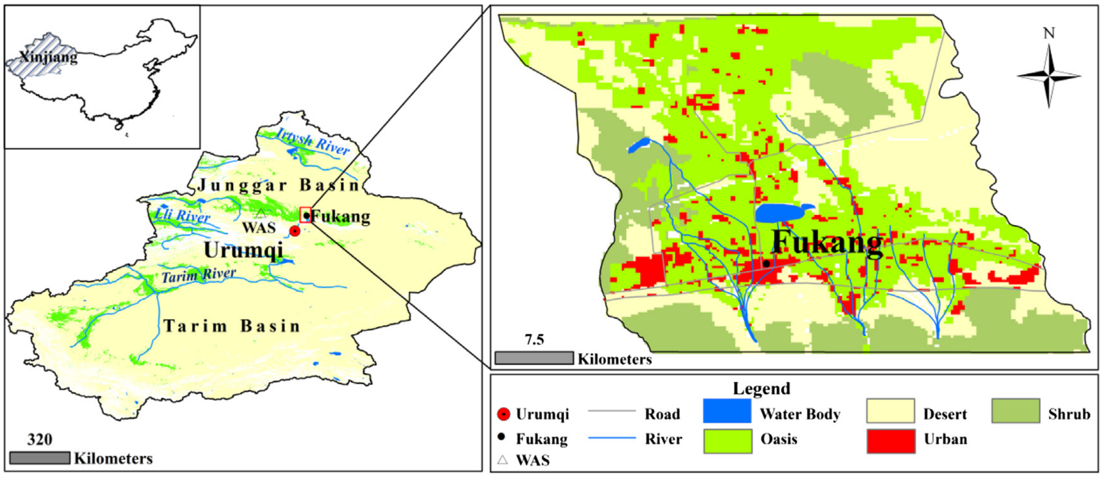

Fig. 1. The location of the study area.

harvest dates were 3 July and 7 September (Huang et al., 2000; Wang and Huang, 1994), respectively. Irrigation was applied five times, and fertilizer was applied four times for both corn and winter wheat during the growing season. The total amounts of irrigation water applied were 552 mm for corn and 720 mm for winter wheat. The total amounts of nitrogen fertilization for the two crops increased from 7.2 kgN ha^{-1} in 1971 to 40 kgN ha^{-1} in 2006. The management inventory data (including time and amount of irrigation and fertilization) were derived from the Fukang National Economic Statistical Yearbook (Fukang Statistic Bureau, 2007) for 1971–2006.

2.4. Model inputs

Oasis-scale simulation required grid-based meteorological, cropland distribution and soil texture maps, as well as practice information on irrigation and fertilization in croplands. To produce an accurate representation of the expansion of croplands, all required spatial input variables were produced at a spatial resolution of 250 m × 250 m.

Meteorological variables, including the maximum, minimum and mean air temperature, precipitation, vapor pressure deficit (VPD), solar radiation and day-length, were generated by interpolating site-recorded meteorological data from 28 sites in the northern Tianshan Mountains, according to the approach of Liston and Elder (2006). The Shuttle Radar Topographic Mission (SRTM) DEM data, which have a spatial resolution of 90 m, were used for spatial interpolation (Jarvis et al., 2008).

The maps of cropland distribution were extracted from Landsat images in 1978 (MSS), 1987 (TM), 1998 (ETM+), and 2006 (TM) by interactive interpretation, and the four cropland maps represented the four decadal periods (1970s, 1980s, 1990s, and early 2000s). The C_3 crop (winter wheat) was distributed in the lower reaches (elevation lower than 500 m), while the C_4 crop (corn) was grown in the upper reaches (elevation higher than 500 m).

Sixty soil samples were collected from thirteen slopes at Sangonghe Catchment in 2006 and were used to generate a regional soil texture map.

2.5. Model description and modifications

In the Biome-BGC model, NPP was calculated as the gross primary production (GPP) minus the sum of maintenance respiration (M_R) and growth respiration (G_R) (Running and Coughlan, 1988). NPP consisted of both aboveground (leaves, stems) and belowground (roots) components. The daily net photosynthate was allocated to leaves (C_L) and roots (C_R) by a leaf/root carbon ratio for grass (Running and Cower, 1991). LAI integrated canopy radiation absorption, water interception, photosynthesis, and litter inputs to detrital pools (White et al., 2000), and thus was a central variable in the Biome-BGC model. The LAI was calculated as the ratio of the leaf carbon mass to the specific leaf area (SLA) in this model.

In this paper, a specific agriculture module was integrated into the current version of the Biome-BGC model (4.1.2) for application to agricultural systems. The agricultural module consists of three main components: phenology, biomass allocation and management (irrigation and fertilization). Crop phenology was incorporated into the Biome-BGC model via daily accumulated temperature, which was also used to control biomass partitioning (Huang et al., 2009). Unlike grass, the crop has grain and stem organs; thus, the aboveground biomass is allocated to the leaf (G_L), stem (C_S) and grain (C_G), while the partitioning coefficients for different organs empirically vary with crop phenology. The phenology stage at any given day, *i*, between planting and maturity is the crop developmental index (DVI; Huang et al., 2009; listed in Appendix A), computed as

$$\mathrm{DVI} = \frac{\sum_{i=1}^{n}(T_i - B)}{\mathrm{AT}} \quad (1)$$

where T_i is daily mean air temperature, B is the minimum temperature for crop development, AT is the total accumulated temperature (degree-days) above the lower limit (B) during the growing season, and n is the length of the growing season in days.

The Biome-BGC model couples the water, carbon and nitrogen cycles. Leaf growth is modified by both leaf water status and nitrogen availability (Running and Cower, 1991). The soil nitrogen concentration is controlled by the decomposition rates of nitrogen (K_{LTC}) in the litter and soil, and K_{LTC} is calculated as a function of soil moisture (W_s) and temperature (T_s) (Running and Cower, 1991). When the soil water content (SWC) exceeds field capacity, the excess soil water is drained and the soil mineralized nitrogen (SMN) occurs leaching. In the revised model, irrigation and fertilization were directly added into the soil compartment. Irrigated water was treated as rainfall without canopy interception and was routed to the soil. The fertilization was treated as the same process by which atmospheric nitrogen deposition is added to the soil mineralized nitrogen.

2.6. Model parameterization and validation

Among the eco-physiological parameters of the Biome-BGC model, those related to phenology, carbon allocation and specific leaf area (SLA) were determined from observations at the WAS site, and the rest were derived from Wang et al. (2005) and White et al. (2000). The twelve site-years of observed data, including LAI, leaf and stem dry matter, crop yields, and pan evaporation were used to validate the performance of the modified model for winter wheat and corn at the WAS site.

The measured crop yields (Y) were converted to carbon mass (NPP) by the following equation (Huang et al., 2007; Lobell et al., 2002):

$$\mathrm{NPP} = \frac{(1-\mathrm{MC}) \times Y \times C}{\mathrm{HI} \times f_{\mathrm{AG}}} \quad (2)$$

where HI is harvest index, defined as the ratio of grain yield to total aboveground biomass; f_{AG} is the root-to-shoot ratio; MC is the moisture content at harvest (expressed as a fraction of soil volume); and C is a conversion factor from biomass to carbon content. The HI was set as an average value of the measurements at the WAS site. The values of C and MC were set to 0.45 and 0.11, respectively (Lobell et al., 2002) for both winter wheat and corn, and the value of f_{AG} was set to 0.11 for winter wheat and 0.09 for corn (Huang et al., 2007).

Actual crop evapotranspiration (ET) was estimated from the measured pan evaporation (E_{pan}) based on the single crop coefficient approach (Allen et al., 1998) and was then compared with the simulated evapotranspiration (Ju et al., 2010; Yang et al., 2011) as follows:

$$\mathrm{ET} = E_{\mathrm{pan}} \times K_{\mathrm{p}} \times K_{\mathrm{c}} \quad (3)$$

where E_{pan} is the pan evaporation (measured by a pan with diameter of 20 cm), and K_p and K_c are the pan and crop coefficients, respectively. The value of K_p was set to 0.7 (Allen et al., 1998), and K_c was set to 0.93 for winter wheat and 1.1 for corn (Liu et al., 2002).

2.7. Simulation experiments

Two simulations were conducted to investigate the individual contributions of climate change and management practices (irrigation and fertilization) to NPP and ET; the results were then compared with the original Biome-BGC results and the observed data at the site scale. In the climate simulation (CLM), only the climate data were included in the modified Biome-BGC model. In the climate and management simulation (CLM + Mana), both climate factors and management practices were used to drive the modified model.

At the catchment scale, four simulation experiments (Table 1) were conducted to examine the responses of total NPP and ET to the changes in oasis expansion, management practices and daily climate in the Sangonghe Oasis from the 1970s through the 2000s. Simulation I (CLM + Mana + LUCC) was designed to simulate total NPP and ET by combining three effects including historical change in climate (1971–2006), management practices (1971–2006) and cropland area (1978, 1988, 1998 and 2006). Simulation II (CLM + Mana) considered cropland area to be unchanged in 1978, but climate and management practices changed between 1971 and 2006. Simulation III (CLM + LUCC) considered changes in both the oasis cropland area and climate from 1971 to 2006, but omitted management practices. Simulation IV (CLM) included forced historical climate change (1971–2006) but omitted management practices and cropland area was in 1978.

Table 1
Design of catchment-scale simulation experiments in the Sangonghe Oasis. CLM, Mana, and LUCC represent climate, management practices, and cropland expansion, respectively. CLM + Mana + LUCC, CLM + Mana, CLM + LUCC, and CLM represent the simulations performed with CLM + Mana + LUCC, CLM + Mana, CLM + LUCC, and CLM, respectively.

	Simulations	Climate	Management	Cropland maps
I	CLM + Mana + LUCC	1971–2006	1971–2006	1978\1988\1998\2006
II	CLM + Mana	1971–2006	1971–2006	1978
III	CLM + LUCC	1971–2006	No	1978\1988\1998\2006
IV	CLM	1971–2006	No	1978

3. Results

3.1. Comparison between simulated and measured biometric variables

Fig. 2 compares the LAI simulation with the modified Biome-BGC model and the measurements for corn (Fig. 2a) and winter wheat (Fig. 2b) at the WAS site. Coefficients of determination (R^2) between the modeled and measured LAI were 0.84 and 0.73 for corn and winter wheat, respectively. Root mean square error (RMSE) values for LAI were 0.75 $m^2\ m^{-2}$ for corn and 1.33 $m^2\ m^{-2}$ for winter wheat. These results indicated that the modified Biome-BGC model agreed well with measured LAI values for both C_4 and C_3 crops; however, model errors differed between crops. For corn, the model slightly overestimated LAI before the jointing stage (LAI $< 2\ m^2\ m^{-2}$). For winter wheat, although agreement between the model and the measurement was poor from heading to flowering (LAI $> 4\ m^2\ m^{-2}$), the majority of the measured LAI values were within one standard deviation of the modeled LAI.

Fig. 3 shows the comparisons between simulated and measured dry mass (measured in carbon) for the leaves and stems. The measured leaf biomass was converted to carbon mass by multiplying by a conversion factor (0.45) to compare with the modeled leaf carbon mass. Coefficients of determination (R^2) between modeled and measured leaf carbon mass were 0.7 for corn (Fig. 3a) and 0.64 for winter wheat (Fig. 3b), respectively. The RMSE values were 31.13 gC m^{-2} and 27.24 gC m^{-2} for corn and winter wheat, respectively. As SLA has been reported to change at different growth stages, the Biome-BGC model showed slightly worse performance for leaf carbon mass than for LAI. For stem carbon mass, the model exhibited satisfactory performance for both corn and winter wheat, although the model overpredicted stem carbon mass during the early growing period. The correlation coefficients between modeled and measured stem dry mass were 0.69 for corn (Fig. 3c) and 0.55 for winter wheat (Fig. 3d), respectively. The RMSE values were 59 gC m^{-2} and 58.5 gC m^{-2} for corn and winter wheat, respectively. The mean model error for both crops was less than 20%.

The comparison between the modeled NPP and the calculated NPP from the measured crop yield is shown in Fig. 4. The model produced good agreement with the measured NPP. The correlation coefficients and RMSE values for corn were 0.76 and 39.46 gC m^{-2} (Fig. 4a), and those for winter wheat were 0.8 and 25.33 gC m^{-2} (Fig. 4b), respectively. The model produced lower NPP for corn (average = 1100 gC m^{-2}) than for winter wheat (average = 700 gC m^{-2}), in agreement with the NPP calculated from the observed yields.

3.2. Comparison between simulated and measured ET

Linear regression analysis between modeled and observed daily ET during the growing season showed good agreements for both corn ($R^2 = 0.84$; Fig. 5a) and winter wheat ($R^2 = 0.74$; Fig. 5b), indicating that the Biome-BGC model could explain more than 70%

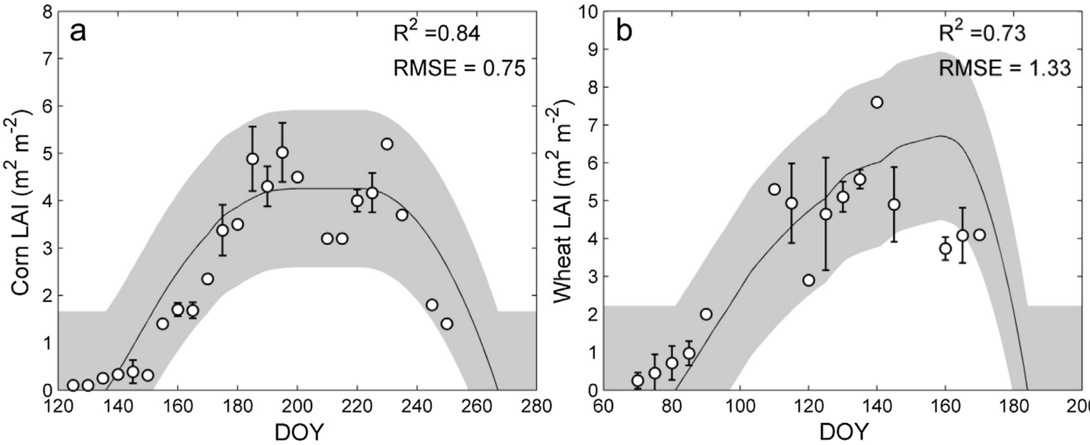

Fig. 2. Observed vs. modeled LAI dynamics for corn (a) and winter wheat (b). Both the observed and modeled LAI are averaged over multiple years from 1995 to 2007. The circle represents the average LAI, and the error bar represents the standard deviation of the observed LAI. The solid line indicates the modeled LAI, and the shaded area indicates the standard deviation of the modeled LAI. R^2 is the square of coefficient of determination, and RMSE is root mean square error in $m^2\ m^{-2}$.

of the variance in the measured evapotranspiration. RMSE values were 0.83 mm and 0.81 mm for corn and winter wheat, respectively.

3.3. *Responses of the simulated NPP and ET to climate change and management practices*

As shown in Fig. 6, the CLM and Original (with the original Biome-BCG model) site-scale simulations, with no management practices, highly underestimated the NPP for both corn (Fig. 6a) and winter wheat (Fig. 6b). The modeled NPP with "CLM" and "Original" accounted for only 19% and 33% of the observed NPP for corn and 5% and 24% of the observations for winter wheat, respectively. These results indicated that management practices contributed significantly to NPP in the oasis croplands. The simulation "CLM + Mana" with the modified Biome-BGC model produced good agreement with observations for both crops.

3.4. *Temporal and spatial patterns of NPP and ET from the 1970s through the 2000s*

The total net primary productivity (TNPP) and total ET (TET) in the catchment were calculated as the sum of annual NPP and ET for

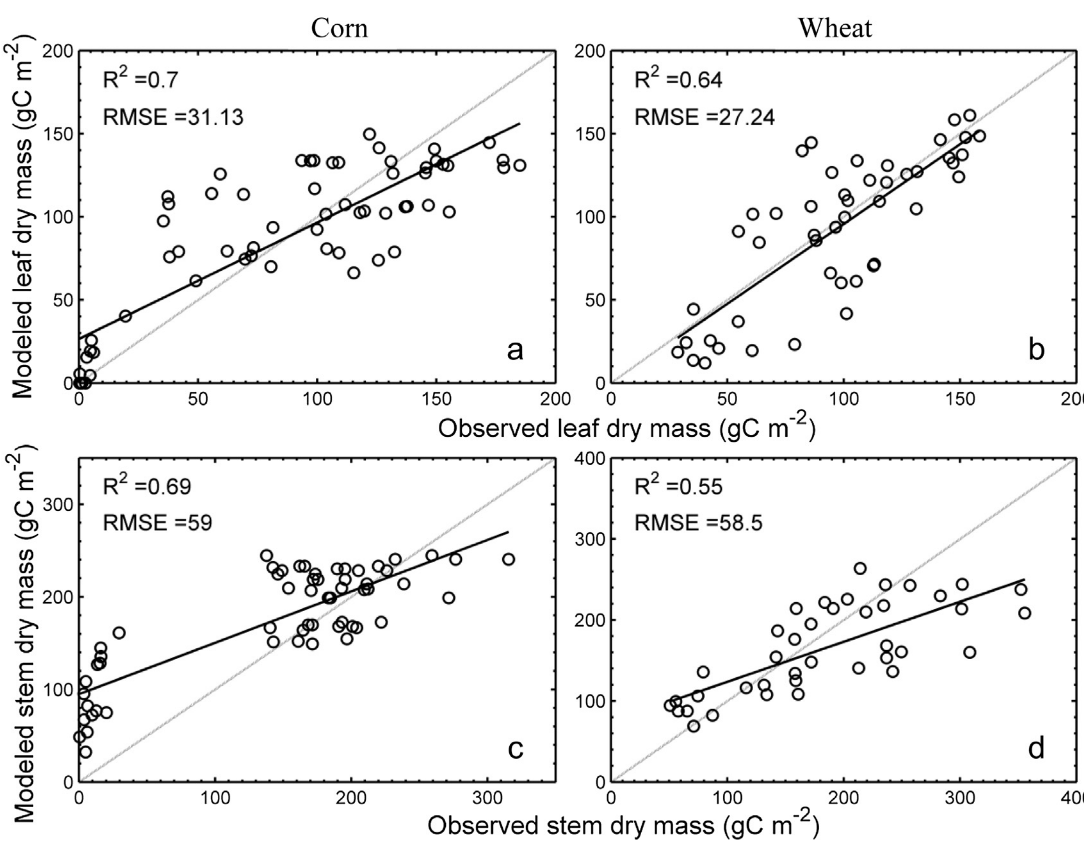

Fig. 3. Observed vs. modeled leaf and stem dry mass for corn (a, c) and winter wheat (b, d) from 1995 to 2007. The dotted line indicates the 1:1 line. The solid line indicates the linear regression.

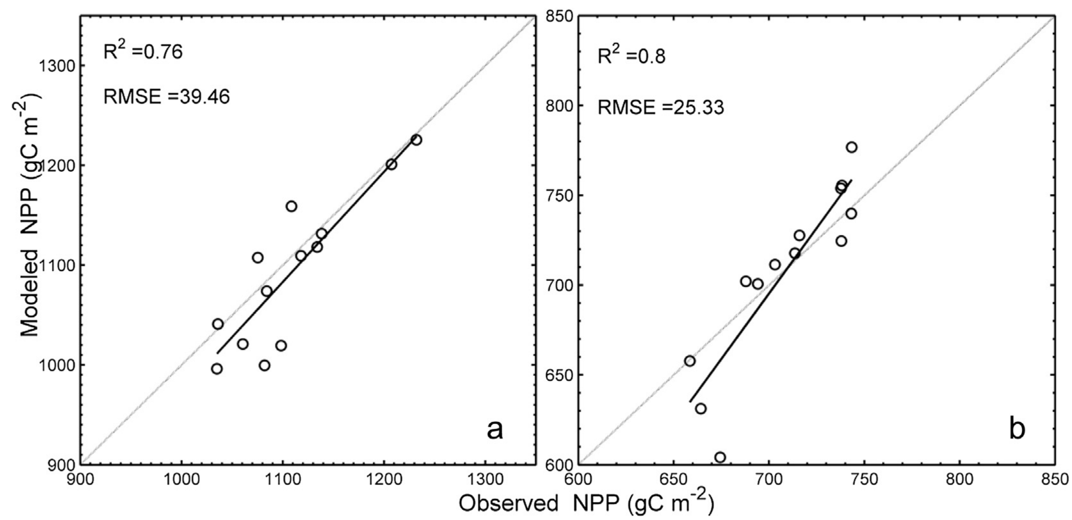

Fig. 4. Observed vs. modeled net primary production (NPP) of corn (a) and winter wheat (b) from 1995 to 2007. The dotted line indicates the 1:1 line. The solid line indicates the linear regression.

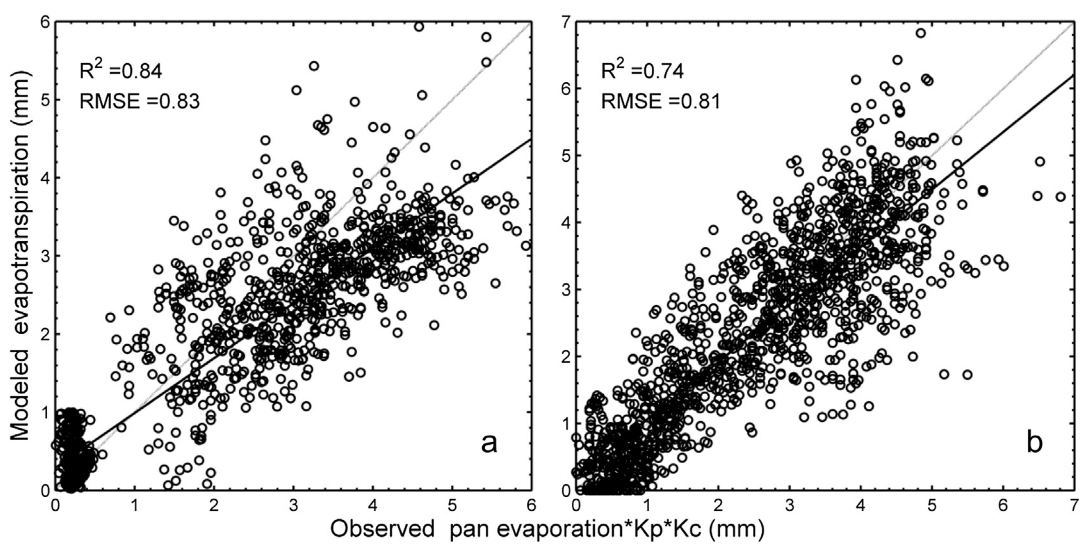

Fig. 5. Observed vs. modeled evapotranspiration (ET) of corn (a) and winter wheat (b) from 1995 to 2007. The dotted line indicates the 1:1 line. The solid line indicates the linear regression.

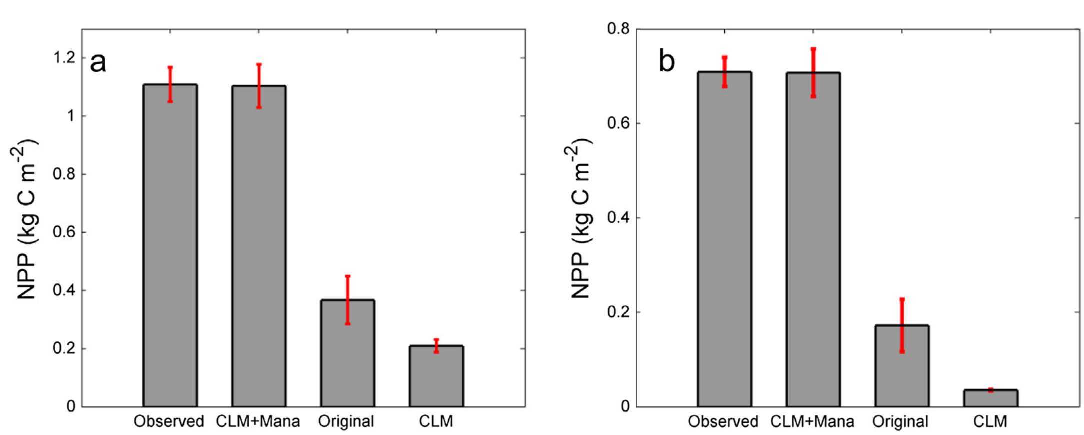

Fig. 6. Observed and simulated net primary production (NPP) for corn (a) and winter wheat (b) at the WAS site from 1995 to 2007. 'Observed' is the calculated value of NPP using Eq. (2). 'Original' represents the simulation performed with the original Biome-BGC model. 'CLM' represents the simulation run with climate only, using the modified Biome-BGC model. 'CLM + Mana' represents the simulation performed with both climate and management practices, using the modified Biome-BGC model.

all crop pixels. The corn TNPP increased from 0.23 PgC $year^{-1}$ in the 1970s (average form 1971–1979) to 0.31 PgC $year^{-1}$ in the early 2000s (average from 2000 to 2006) (Fig. 7a). The winter wheat TNPP increased much more, from 0.08 PgC $year^{-1}$ to 0.24 PgC $year^{-1}$ from the 1970s through the 2000s (Fig. 7a). The rates of TNPP increased by 19.7%, 13.6%, and 1.5% for corn and 14.2%, 78.2%, and 51.4% for winter wheat during the 1970s, 1980s, and 2000s, respectively. Consequently, the catchment TNPP increased by 81.8% from the 1970s through the 2000s; 34.4% of the increase was contributed by corn, and the remaining 65.5% was contributed by winter wheat.

Like the catchment TNPP, TET increased by 89.4% from 1.04×10^8 m^3 to 1.87×10^8 m^3 between the 1970s and the early 2000s. The TET for winter wheat increased from 0.43×10^8 m^3 to 1.10×10^8 m^3, while TET for corn increased by a relatively small amount, from 0.60×10^8 m^3 to 0.87×10^8 m^3, from the 1970s through the 2000s (Fig. 7b). At the catchment scale, the winter wheat contributed 71.7% of increased TET, while corn contributed 28.3% from the 1970s through the 2000s.

Fig. 7c shows the changes in cropland area for both corn and winter wheat in the Sangonghe Catchment. The area of corn increased by 22.0% and that of winter wheat increased by 78.0% from the 1970s through the 2000s. The contributions of the changes in cropland area (LUCC), management practices (Mana), climate (CLM) and their interactions to regional TNPP and TET indicate that the increases in cropland area explain 40.3% and 60.5% of the increased regional TNPP and TET, respectively (Fig. 7d). The Mana explained 46.1% and 13.3% of the increased TNPP and TET, respectively, whereas the CLM contributed only 1.8% and 4.7%, respectively. The interactions between CLM and Mana explained 10% and 16.8% of the increased TNPP and TET, the interactions between Mana and LUCC explained 1.8% and 4.7%, and we assumed no interactions between CLM and LUCC. The results demonstrated that human activities, especially agricultural oasis expansion, played a significant role in increasing agro-ecosystem productivity (NPP) and water consumption (ET) compared to climate change in the Sangonghe Oasis.

Fig. 8 shows the spatial distribution of NPP and ET changes from the 1970s through the 2000s in the Sangonghe Oasis. The upper (southern) region of the oasis was called the “old oasis” and experienced less expansion during the past forty years; NPP and ET showed only slight increases. The lower (northeastern) region of the oasis experienced greater increases in NPP and ET; this newly cultivated cropland was converted from desert shrub between 1970 and the early 2000s. ET increased more than the NPP in all oasis croplands, especially in the 1980s and 1990s. Overall, the old oasis contributed only 12.2% and 22% of the total increased NPP and ET, respectively, whereas the newly developed oasis contributed majority of the increased NPP and ET in Sangonghe Oasis from the 1970s through the 2000s.

4. Discussion

The impacts of the change in climatic factors (e.g., temperature, net radiation, wind speed and relative humidity, etc.) on crop NPP and ET have been widely examined (Dinpashoh et al., 2011; Donohue et al., 2010; Jhajharia et al., 2011; McVicar et al., 2011, 2010). Land-use change and agricultural management practices

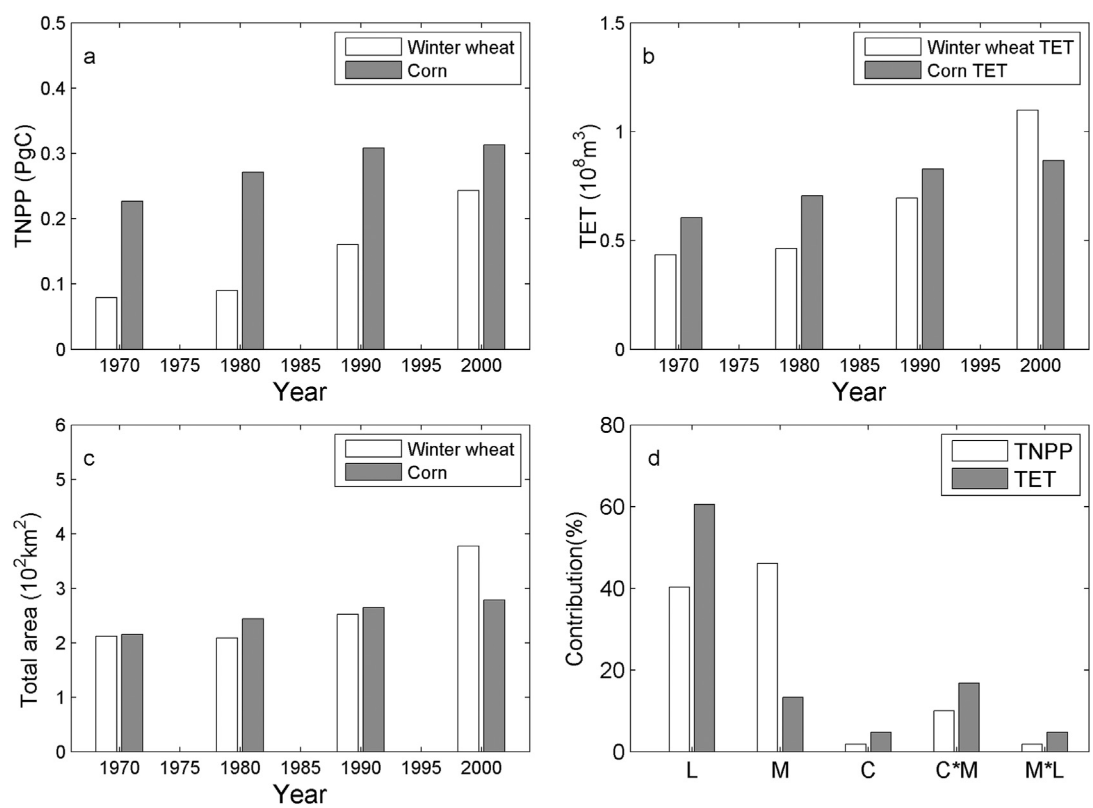

Fig. 7. Total net primary productivity (TNPP; PgC; a), total evapotranspiration (TET; 10^8 m^3; b), and total area (10^2 km^2; c) of corn and winter wheat between 1970 and the early 2000s. The contributions (%) of changes in cropland area (L), management practices (M), climate change (C) and their interactions (including C × M and M × L) on the changes in TNPP and TET from 1971 to 2006 (d). C × M indicates the interactions between C and M, and M × L indicates the interactions between M and L. We assumed no interactions between C and L (C × L = 0).

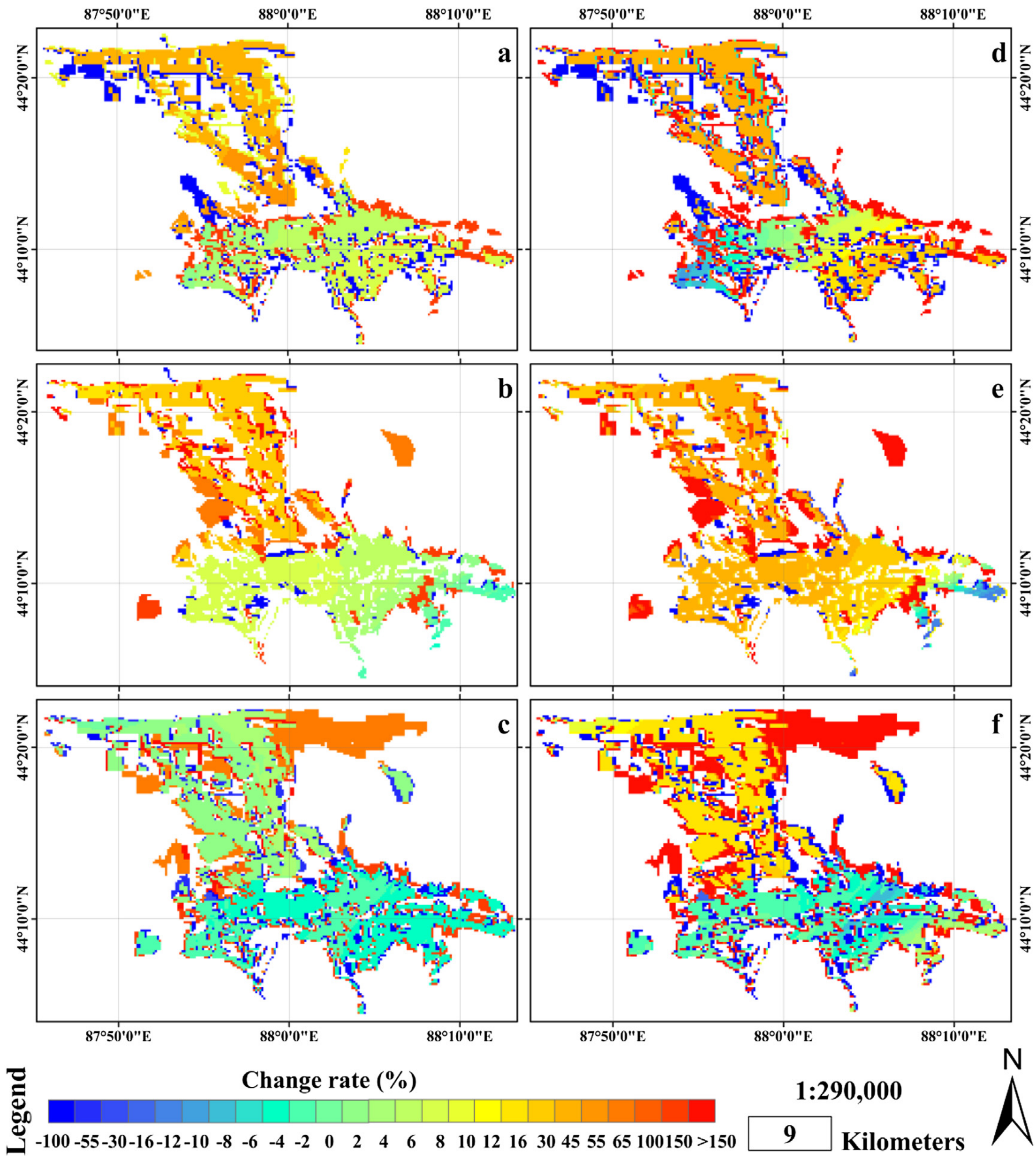

Fig. 8. Rate of change (defined as the ratio of the difference between the values at the end and start year to the value at the start year) in mean annual net primary production and evapotranspiration during the growing season in association with the combined effects of oasis expansion, management practices and climate change from the 1970s through the 1980s (a for NPP, d for ET), 1980s-1990s (b for NPP, e for ET), and 1990s-2000s (c for NPP, f for ET).

(e.g., irrigation and fertilization) have been considered important to NPP and ET in cropland ecosystems (Li et al., 2011; Ren et al., 2012; Zhang et al., 2011). Climate change, land-use change and management practices have been captured by ecosystem models (Bondeau et al., 2007; Ciais et al., 2011; Huang et al., 2009; Li et al., 2011; Ren et al., 2012). As in other studies, we found that management practices (irrigation and fertilization) were among the most important factors for maintaining crop productivity at the site scale (Huang et al., 2007; Ren et al., 2012). In a regional simulation, we also found that area changes in the agricultural oasis were the dominant factor modifying the spatial distributions of NEE and ET, and that cropland conversion from natural vegetation would increase NPP.

Variation in water resources is a crucial factor in agriculture, which in Xinjiang relies heavily on irrigation (Zhang et al., 2010). Shi et al. (2007) reported that the average annual precipitation from 1987 to 2000 was 22% higher than that from 1961 to 1986 in Xinjiang; however, the irrigated cropland covering 90% of the total cropland area increased by 147% from 1951 to 2000 (Xinjiang Statistic Bureau, 2005). The annual available water for agriculture was 4.07×10^{10} m^3, but the annual water consumption for irrigated cropland was 4.4×10^{10} to 4.6×10^{10} m^3 (Fan et al., 2013). Water resources for the expansion of cropland are limited in Xinjiang. The rapid and substantial expansion of cropland also might have significant impacts on regional carbon and hydrological cycles, and the ecosystem stability and sustainable development of the oasis are highly threatened (Jia et al., 2004; Shen and Chen. 2010; Wang et al., 2007; Zhang et al., 2003). No comprehensive, integrated, and quantitative analysis of the effects of climate change, management and land-use change on the regional total NPP and ET has been reported in Xinjiang. This paper was aimed at filling this knowledge gap. The conclusions of this regional simulation study might have important implications for maintaining the stability of the oasis and reconciling the conflict over water resources between supply and demand in arid regions.

Although some specific agricultural processes have been incorporated into the Biome-BGC model and the simulated LAI and biometric variables were satisfactory, the uncertainties in carbon imports and exports caused by changes in land use from desert shrublands to croplands were not considered in the current modified model. Previous studies suggested that land-use change caused carbon release via the conversion from natural vegetation to crops (Houghton and Goodale, 2004; Mann, 1986). The carbon content in the soil profile in newly cultivated croplands later increased due to optimized land-management strategies such as fertilizer/irrigation application and rotation (Houghton et al., 2010). The uncertainties of irrigation evaporation were not considered in estimates of soil evaporation in this modified model. Howell (2003) reported that the irrigation efficiency ranged from 75% to 90% and that 10–25% of the surface irrigation was lost to evaporation in the field. Drainage was the primary component of loss to irrigation (Howell, 2003) and could be estimated by the recharge coefficient and the amounts of irrigation and effective precipitation (Sun et al., 2010).

A follow-up study will include the effect of land-use change on the net ecosystem exchange of carbon and the effect of irrigation efficiency on the exchange of water into the modified Biome-BGC model and conduct further comprehensive assessments of the effects of climate change and human activities on regional carbon and hydrological cycles in oasis croplands.

5. Conclusion

In this study, the original Biome-BGC model was modified by integrating major agricultural processes (phenology, biomass allocation, irrigation and fertilization practices). The modified Biome-BGC model has been verified for LAI, biometric variables, NPP, and ET. Simulation experiments indicated that management practices had much stronger effects on NPP and ET than did climate factors at the site scale; however, the increase in the area of agricultural oases, i.e., oasis expansion, was the significant factor in increasing the catchment total NPP and ET between the 1970s and the early 2000s. Our modeling research quantified the contributions of natural factors, human activities and their interactions to regional carbon and hydrological cycles at the catchment scale. The simulated TNPP increased significantly by 81.8%, and TET increased by 89.4%. Under a changing climate, human activities might lead to water shortages in the oasis croplands of northwest China.

Acknowledgment

This research was funded by the National Program on Key Basic Research Project of China (Grant No. 2009CB825105), the "Hundred Talent" project of Chinese Academy of Sciences granted to L. Li (Grant No. Y174051001), and the Natural Science Foundation of China (Grant No. 41101101). The Biome-BGC model (version 4.1.2) was provided by Peter Thornton at the National Centre for Atmospheric Research (NCAR), and by the Numerical Terra dynamic Simulation Group (NTSG) at the University of Montana. We are grateful to two USDA-ARS scientists for generously providing language editing in the revision of the manuscript.

Appendix A. Partitioning coefficients of photosynthate to leaf (P_L), stem (P_S) and grain (P_G) for corn and winter wheat.

DVI	Corn			Winter wheat		
	P_L	P_S	P_G	P_L	P_S	P_G
0.0	0.70	0.30	0.00	0.67	0.33	0.00
0.1	0.70	0.30	0.00	0.67	0.33	0.00
0.2	0.70	0.30	0.00	0.67	0.33	0.00
0.3	0.70	0.30	0.00	0.67	0.33	0.00
0.4	0.70	0.30	0.00	0.63	0.37	0.00
0.5	0.66	0.33	0.00	0.50	0.50	0.00
0.6	0.50	0.50	0.00	0.40	0.60	0.00
0.7	0.34	0.66	0.00	0.30	0.70	0.00
0.8	0.20	0.80	0.00	0.20	0.80	0.00
0.9	0.10	0.90	0.00	0.10	0.90	0.00
1.0	0.00	0.00	1.00	0.00	0.00	1.00

The crop developmental index (DVI) has values of 0 at crop emergence and 1 at heading (for winter wheat) and at silking (for corn).

Appendix B. Performance statistics of the modified Biome-BGC model for winter wheat and corn at the WAS site. R^2 is the square of the coefficient of determination; RMSE is the root mean square error; and S is the slope of the linear regression between the modeled and observed values.

Variables	Unit	Corn			Winter wheat		
		R^2	RMSE	SLOP	R^2	RMSE	SLOP
LAI	$m^2\ m^{-2}$	0.84	0.75	0.82	0.73	1.33	1.02
Leaf dry mass	$gC\ m^{-2}$	0.7	31.13	0.96	0.64	27.24	0.7
Stem dry mass	$gC\ m^{-2}$	0.69	59	0.49	0.55	58.5	0.56
NPP	$gC\ m^{-2}$	0.76	39.46	1.1	0.8	25.33	1.46
ET	m^3	0.84	0.83	0.7	0.74	0.81	0.86

References

Aggarwal, P.K., Kalra, N., Chander, S., Pathak, H., 2006. InfoCrop: a dynamic simulation model for the assessment of crop yields, losses due to pests, and environmental impact of agro-ecosystems in tropical environments. I. Model description. Agric. Syst. 89, 1–25.

Allen, R.G., Pereira, L.S., Raes, D., Smith, M., 1998. Crop Evapotranspiration-guidelines for Computing Crop Water Requirements. Irrigation and Drain, Paper No. 56. FAO, Rome, pp. 156–166.

Bradford, J.B., Hicke, J.A., Lauenroth, W.K., 2005. The relative importance of light-use efficiency modifications from environmental conditions and cultivation for estimation of large-scale net primary productivity. Remote Sens. Environ. 96, 246–255.

Bondeau, A., Smith, P.C., Zaehle, S., Schaphoff, S., Lucht, W., Cramer, W., Gerten, D., Lotze-campen, H., Müller, C., Reichstein, M., Smith, C., 2007. Modelling the role of agriculture for the 20th century global terrestrial carbon balance. Glob. Chang. Biol. 13, 679–706.

Ciais, P., Gervois, S., Vuichard, N., Piao, S.L., Viovy, N., 2011. Effects of land use change and management on the European cropland carbon balance. Glob. Chang. Biol. 17, 320–338.

Chiesi, M., Masellia, F., Moriondob, M., Fibbia, L., Bindib, M., Running, S.W., 2007. Application of Biome-BGC to simulate Mediterranean forest processes. Ecol. Model. 206, 179–190.

Churkina, G., Zaehle, S., Hughes, J., Viovy, N., Chen, Y., Jung, M., Heumann, B.W., Ramankutty, N., Heimann, M., Jones, C., 2010. Interactions between nitrogen deposition, land cover conversion, and climate change determine the contemporary carbon balance of Europe. Biogeosciences 7, 2749–2764. http://dx.doi.org/10.5194/bg-7-2749-2010.

Clark, D.B., Mercado, L.M., Sitch, S., Jones, C.D., Gedney, N., Best, M.J., Pryor, M., Rooney, G.G., Essery, R.L.H., Blyth, E., Boucher, O., Harding, R.J., Cox, P.M., 2011. The Joint UK Land Environment Simulator (JULES), model description – part 2: carbon fluxes and vegetation. Geosci. Model Dev. 4, 701–722. http://dx.doi.org/10.5194/gmdd-4-701-2011.

Chen, X., 2008. Land Use/cover Change in Arid Areas in China. Science Press, Beijing, pp. 480–490 (in Chinese).

De Noblet-Ducoudré, N., Gervois, S., Ciais, P., Viocy, N., Brisson, N., Seguin, B., Perrier, A., 2004. Coupling the Soil-Vegetation-Atmosphere-Transfer scheme ORCHIDEE to the agronomy model STICS to study the influence of croplands on the European carbon and water budgets. Agronomie 24, 1–11.

Dinpashoh, Y., Jhajharia, D., Fakheri-Fard, A., Singh, V.P., Kahya, E., 2011. Trends in reference crop evapotranspiration over Iran. J. Hydrol. 399, 422–433.

Di Vittorio, A.V., Anderson, R.S., White, J.D., Miller, N.L., Running, S.W., 2010. Development and optimization of an Agro-BGC ecosystem model for C_4 perennial grasses. Ecol. Model. 221, 2038–2053.

Donohue, R.J., McVicar, T.R., Roderick, M.L., 2010. Assessing the ability of potential evaporation formulations to capture the dynamics in evaporative demand within a changing climate. J. Hydrol. 386, 186–197.

Fan, Z.L., Wu, S.X., Wu, Y., Zhang, P., Zhao, X.F., Zhang, J., 2013. The land reclamation in Xinjiang since the founding of new China. J. Nat. Resour. 28, 713–720 (in Chinese).

Foley, J.A., DeFries, R.S., Asner, G.P., Barford, C., Bonan, G., Carpenter, S.R., Chapin, F.S., Coe, M.T., Daily, G.C., Gibbs, H.K., Helkowski, J.H., Holloway, T., Howard, E.A., Kucharik, C.J., Monfreda, C., Patz, J.A., Prentice, I.C., Ramankutty, N., Snyde, P.K., 2005. Global consequences of land use. Science 309, 570–574.

Field, C.B., Randerson, J.T., Malmstrom, C.M., 1995. Global net primary production: combining ecology and remote sensing. Remote Sens. Environ. 51, 74–88.

Fukang Statistic Bureau, 2007. Fukang National Economic Statistical Yearbook. Xinjiang Statistics Press, Xinjiang (In Chinese).

Gervois, S., De Noblet-Ducoudré, N., Viovy, N., Viocy, N., Ciais, P., 2004. Including croplands in a global biosphere model: methodology and evaluation at specific sites. Earth Interact. 8, 1–25.

Graf, B., Rakotobe, O., Zahner, P., Delucchi, V., Gutierrez, A.P., 1990. A simulation model for the dynamics of rice growth and development: part I-the carbon balance. Agric. Syst. 32, 341–365.

Hoof, C.V.D., Hanert, E., Vidale, P.L., 2011. Simulating dynamic crop growth with an adapted land surface model-JULES-SUCROS: model development and validation. Agric. For. Meteorol. 151, 137–153.

Howell, T.A., 2003. Irrigation efficiency. In: Dekker, M. (Ed.), Encyclopedia of Water Science, New York, pp. 467–472.

Houghton, R.A., 2010. How well do we know the flux of CO_2 from land-use change? Tellus 62B, 337–351.

Houghton, R.A., Goodale, C.L., 2004. Effects of land-use change on the carbon balance of terrestrial ecosystems. In: DeFries, R.S., Asner, G.P., Houghton, R.A. (Eds.), Ecosystems and Land Use Change. American Geophysical Union, Washington, DC, pp. 85–98.

Houghton, R.A., Hackler, J.L., 2003. Sources and sinks of carbon from landuse change in China. Glob. Biogeochem. Cycles 17, 1034.

Huang, Y., Yu, Y.Q., Zhang, W., Sun, W.J., Liu, S.L., Jiang, J., Wu, J.S., Yu, W.T., Wang, Y., Yang, Z.F., 2009. Agro-C: a biogeophysical model for simulating the carbon budget of agroecosystems. Agric. For. Meteorol. 149, 106–129.

Huang, Y., Zhang, W., Sun, W.J., Zhang, X.H., 2007. Net primary production of Chinese croplands from 1950 to 1999. Ecol. Appl. 17, 692–701.

Huang, J.F., Wang, X.Z., Cai, C.X., 2000. Research on winter wheat phenology and climate in Xinjiang. Chin. J. Agrometeorol. 21, 14–19 (in Chinese).

Hu, R.J., Jiang, F.Q., Wang, Y.J., 2010. To have a correct understanding of the stability of oasis in arid lands of China. Arid Zone Res. 27, 319–323 (in Chinese).

Jarvis, A., Reuter, H.I., Nelson, A., Guevara, E., 2008. Hole-filled SRTM for the Globe Version 4 available from: the CGIAR-CSI SRTM 90m Database http://srtm.csi.cgiar.org.

Jia, B.Q., Zhang, Z.Q., Ci, L.J., 2004. Oasis land-use dynamics and its influence on the oasis environment in Xinjiang, China. J. Arid Environ. 56, 11–26.

Jhajharia, D., Dinpashoh, Y., Kahya, E., Singh, V.P., Fakheri-Fard, A., 2011. Trends in reference evapotranspiration in the humid region of northeast India. Hydrol. Process.. http://dx.doi.org/10.1002/hyp.8140.

Ju, W.M., Gao, P., Wang, J., Zhou, Y.L., Zhang, X.H., 2010. Combining an ecological model with remote sensing and GIS techniques to monitor soil water content of croplands with a monsoon climate. Agric. Water Manag. 97, 1221–1231.

Krinner, G., Viovy, N., De Noblet-Ducoudré, N., Ogée, J., Polcher, J., Friedlingstein, P., Ciais, P., Sitch, S., Prentice, I.C., 2005. A dynamic global vegetation model for studies of the coupled atmosphere-biosphere system. Glob. Biogeochem. Cycles 19, GB1015. http://dx.doi.org/10.1029/2003GB002199.

Kucharik, C.J., 2003. Evaluation of a process-based agro-ecosystem model (Agro-IBIS) across the U.S. Corn Belt: simulations of the interannual variability in maize yield. Earth Interact. 7, 1–33.

Kucharik, C.J., Brye, K.R., 2003. Integrated biosphere simulator (IBIS) yield and nitrate loss predictions for Wisconsin maize receiving varied amounts of nitrogen fertilizer. J. Environ. Qual. 32, 247–268.

Li, L., Vuichard, N., Viovy, N., Ciais, P., Wang, T., Ceschia, E., Jans, W., Wattenbach, M., Béziat, P., Gruenwald, T., Lehuger, S., Bernhofer, C., 2011. Importance of crop varieties and management practices: evaluation of a process-based model for simulating CO_2 and H_2O fluxes at five European maize (*Zea mays* L.) sites. Biogeosciences 8, 1721–1736. http://dx.doi.org/10.5194/bg-8-1721-2011.

Lieth, H., 1975. Modelling the primary productivity of the world. In: Lieth, H., Whittaker, R.H. (Eds.), Primary Productivity of the Biosphere. Springer-Verlag, Berlin, pp. 237–263.

Liston, G.E., Elder, K., 2006. A meteorological distribution system for high-resolution terrestrial modeling. J. Hydromteorol. 7, 217–234.

Liu, C.M., Zhang, X.Y., Zhang, Y.Q., 2002. Determination of daily evaporation and evapotranspiration of winter wheat and maize by large-scale weighing lysimeter and micro-lysimeter. Agric. For. Meteorol. 111, 109–120.

Lobell, D.B., Hicke, J.A., Asner, G.P., Field, C.B., Tucker, C.J., Los, S.O., 2002. Satellite estimates of productivity and light use efficiency in United States agriculture, 1982-1998. Glob. Chang. Biol. 8, 1–15.

Luo, G.P., Zhou, C.H., Chen, X.,L.,Y., 2008. A methodology of characterizing status and trend of land changes in oases: a case study of Sangong River watershed, Xinjiang, China. J. Environ. Manag. 88, 775–783.

Ma, S.X., Churkina, G., Wieland, R., Gesslera, A., 2011. Optimization and evaluation of the ANTHRO-BGC model for winter crops in Europe. Ecol. Model. 222, 3662–3679.

Mann, L.K., 1986. Changes in soil carbon storage after cultivation. Soil Sci. 142, 279–288.

McVicar, T.R., Roderick, M.L., Donohue, R.J., Li, L.T., Van Niel, T.G., Thomas, A., Grieser, J., Jhajharia, D., Himri, Y., Mahowald, N.M., Mescherskaya, A.V., Kruger, A.C., Rehman, S., Dinpashoh, Y., 2011. Global review and synthesis of trends in observed terrestrial near-surface wind speeds: implications for evaporation. J. Hydrol. 416–417, 182–205.

McVicar, T.R., Van Niel, T.G., Roderick, M.L., Li, L.T., Mo, X.G., Zimmermann, N.E., Schmatz, D.R., 2010. Observational evidence from two mountainous regions that near-surface wind speeds are declining more rapidly at higher elevations than lower elevations: 1960-2006. Geophys. Res. Lett. 37, L06402.

Mu, Q.Z., Zhao, M.S., Running, S.W., Liu, M.L., Tian, H.Q., 2008. Contribution of increasing CO_2 and climate change to the carbon cycle in China's ecosystems. J. Geophys. Res. 113, G01018. http://dx.doi.org/10.1029/2006JG000316.

Okin, G.S., Gillettebm, D.A., Herrickc, J.E., 2006. Multi-scale controls on and consequences of aeolian processes in landscape change in arid and semi-arid environments. J. Arid Environ. 65, 253–275.

Parton, W.J., Hartman, M.D., Ojima, D.S., Schimel, D., 1998. DAYCENT and its land surface submodel: description and testing. Glob. Planet. Chang. 19, 35–48.

Potter, C.S., Randerson, J.T., Field, C.B., Matson,.A., Vitousek, P.M., Mooney, H.A., Klooster, S.A., 1993. Terrestrial ecosystem production: a process model based on global satellite and surface data. Glob. Biogeochem. Cycles 7, 811–842.

Ren, W., Tian, H.Q., Tao, B., Huang, Y., Pan, S.F., 2012. China's crop productivity and soil carbon storage as influenced by multifactor global change. Glob. Chang. Biol. 18, 2945–2957.

Running, S.W., Hunt, R.E., 1993. Generalization of a forest ecosystem process model for other biomes, Biome-BGC, and an application for global-scale models. In: Ehleringer, J.R., Field, C.B. (Eds.), Scaling Physiologic Processes: Leaf to Globe. Academic Press, CA San Diego, pp. 141–158.

Running, S.W., Cower, S.W., 1991. FOREST-BGC, A general model of forest ecosystem processes for regional applications. II. Dynamic carbon allocation and nitrogen budgets. Tree Physiol. 9, 147–160.

Running, S.W., Coughlan, J.C., 1988. A general model of forest ecosystem processes for regional applications. I. hydrologic balance, canopy gas exchange and primary production processes. Ecol. Model. 42, 125–154.

Shen, Y., Chen, Y., 2010. Global perspective on hydrology, water balance, and water resources management in arid basins. Hydrol Process. 24, 129–135.

Shi, Y.F., Shen, Y.P., Kang, E.S., et al., 2007. Recent and future climate change in northwest China. Clim. Chang. 80, 379–393.

Sun, H.Y., Shen, Y.J., Yu, Q., Flerchinger, G.N., Zhang, Y.Q., 2010. Effect of precipitation change on water balance and WUE of the winter wheat-summer maize rotation in the North China Plain. Agric. Water Manag. 97, 1139–1145.

Tian, H.Q., Lu, C.Q., Chen, G.S., Xu, X.F., Liu, M.L., Ren, W., Tao, B., Sun, G., Pan, S.F., Liu, J.Y., 2011. Climate and land use controls over terrestrial water use efficiency in monsoon Asia. Ecohydrology 4, 322–340.

Turner, D.P., Ritts, W.D., Law, B.E., Cohen, W.B., Yang, Z., Hudiburg, T., et al., 2007. Scaling net ecosystem production and net biome production over a heterogeneous region in the western United States. Biogeosciences 4, 597–612.

Ueyama, M., Ichii, K., Hirata, R., Takagi, K., Asanuma, J., Machimura, T., Nakai, Y., Ohta, T., Saigusa, N., Takahashi, Y., Hirano, T., 2010. Simulating carbon and water cycles of larch forests in East Asia by the Biome-BGC model with AsiaFlux data. Biogeosciences 7, 959–977.

Vetter, M., Churkina, G., Jung, M., Reichstein, M., Zaehle, S., Bondeau, A., Chen, Y., Ciais, P., Feser, F., Freibauer, A., Geyer, R., Jones, C., Papale, D., Tenhunen, J., Tomelleri, E., Trusilova, K., Viovy, N., Heimann, M., 2008. Analyzing the causes and spatial pattern of the European 2003 carbon flux anomaly using seven models. Biogeosciences 5, 561–583.

Vuichard, N., Ciais, P., Belelli, L., Smith, P., Valentini, R., 2008. Carbon sequestration due to the abandonment of agriculture in the former USSR since 1990. Glob. Biogeochem. Cycles 22, 1–8.

Wang, T., 2010a. Some issues on oasification study in China. J. Desert Res. 30, 994–998 (in Chinese).

Wang, T., 2010b. Some issues on oasification study in China. J. Desert Res. 30, 995–998 (in Chinese).

Wang, Y.G., Xiao, D.N., Li, Y., Li, X.Y., 2008. Soil salinity evolution and its relationship with dynamics of groundwater in the oasis of inland river basins: case study from the Fubei region of Xinjiang Province, China. Environ. Monit. Assess. 140, 291–302.

Wang, Y.G., Xiao, D.N., Li, Y., 2007. Temporal-spatial change in soil degradation and its relationship with landscape types in a desert-oasis ecotone: a case study in the Fubei region of Xinjiang Province, China. Environ. Geol. 51, 1019–1028.

Wang, Q.X., Masataka, W., Zhu, O.Y., 2005. Simulation of water and carbon fluxes using Biome-BGC model over crops in China. Agric. For. Meteorol. 131, 209–224.

Wang, Y.X., Zhang, X.L., 1999. Study on oasis regional system and the spatial envelopment. Arid Land Geogr. 22, 62–68 (in Chinese).

Wang, X.Z., Huang, J.F., 1994. Research on maize phenology and climate changes in Xinjiang. Maize Sci. 2, 20–26 (in Chinese).
White, M.A., Thornton, P.E., Running, S.W., Nemani, R.R., 2000. Parameterization and sensitivity analysis of the Biome-BGC terrestrial ecosystem model: net primary production controls. Earth Interact. 3, 1–85.
Xinjiang Statistic Bureau, 2005. Xinjiang 50 Years. China statistic press, Beijing (in Chinese).
Yang, X., Chen, C., Luo, Q., Li, L., Yu, Q., 2011. Climate change effects on wheat yield and water use in oasis cropland. Int. J. Plant Prod. 5, 83–94.
Zhang, X.Y., Chen, S.Y., Sun, H.Y., Shao, L.W., Wang, Y.Z., 2011. Changes in evapotranspiration over irrigated winter wheat and maize in North China Plain over three decades. Agric. Water Manag. 98, 1097–1104.
Zhang, Q., Xu, C.Y., Tao, H., Jiang, T., Chen, Y.D., 2010. Climate changes and their impacts on water resources in the arid regions: a case study of the Tarim River basin, China. Stoch. Environ. Res. Risk A 24, 349–358.
Zhang, H., Wu, J.W., Zheng, Q.H., Yu, Y.J., 2003. A preliminary study of oasis evolution in the Tarim Basin, Xinjiang, China. J. Arid Environ. 55, 545–553.